Targeting Intestinal Inflammation With CD98 siRNA/PEI–loaded Nanoparticles

Hamed Laroui[1], Duke Geem[2], Bo Xiao[1], Emilie Viennois[1], Poonam Rakhya[1], Timothy Denning[2] and Didier Merlin[1,3]

[1]Department of Chemistry and Biology, Center for Diagnostics and Therapeutics, Georgia State University, Atlanta, Georgia, USA; [2]Department of Pathology, School of Medicine, Emory University, Atlanta, Georgia, USA; [3]Veterans Affairs Medical Center, Decatur, Georgia, USA

Intestinal CD98 expression plays a crucial role in controlling homeostatic and innate immune responses in the gut. Modulation of CD98 expression in intestinal cells therefore represents a promising therapeutic strategy for the treatment and prevention of inflammatory intestinal diseases, such as inflammatory bowel disease. Here, the advantages of nanoparticles (NPs) are used, including their ability to easily pass through physiological barriers and evade phagocytosis, high loading concentration, rapid kinetics of mixing and resistance to degradation. Using physical chemistry characterizations techniques, CD98 siRNA/polyethyleneimine (PEI)–loaded NPs was characterized (diameter of ~480 nm and a zeta potential of −5.26 mV). Interestingly, CD98 siRNA can be electrostatically complexed by PEI and thus protected from RNase. In addition, CD98 siRNA/PEI–loaded NPs are nontoxic and biocompatible with intestinal cells. Oral administration of CD98/PEI-loaded NPs encapsulated in a hydrogel reduced CD98 expression in mouse colonic tissues and decreased dextran sodium sulfate–induced colitis in a mouse model. Finally, flow cytometry showed that CD98 was effectively downregulated in the intestinal epithelial cells and intestinal macrophages of treated mice. Finally, the results collectively demonstrated the therapeutic effect of "hierarchical nano-micro particles" with colon-homing capabilities and the ability to directly release "molecularly specific" CD98 siRNA in colonic cells, thereby decreasing colitis.

Received 17 April 2013; accepted 3 September 2013; advance online publication 26 November 2013. doi:10.1038/mt.2013.214

INTRODUCTION

Inflammatory bowel disease (IBD), which includes ulcerative colitis and Crohn's disease, is a chronic debilitating inflammatory condition. The existing effective and targeted treatments are limited by significant systemic side effects arising from the need for high and/or systemic doses.[1,2] In the development of therapeutic strategies, one major drawback has been the inability to target drugs in sufficient quantities to the site of inflammation, which would theoretically maximize the local drug concentration while minimizing systemic side effects. Furthermore, organs of the gastrointestinal tract (particularly the colon) differ in their drug absorption properties, and it is difficult to deliver a drug to the colon with minimal digestive enzyme degradation and/or systemic absorption.

IBD has been strongly correlated with CD98 expression levels in humans[3] and in a mouse model.[4] CD98 is a cell-surface amino-acid transporter formed by covalent linkage of the CD98 heavy chain (CD98hc) with several different light chains. It was recently shown to function as a β1-integrin regulator.[5,6] Our studies and other groups have shown that proinflammatory cytokines can upregulate CD98 expression in intestinal epithelial cells (IECs),[7–9] and CD98 is highly expressed in epithelial and immune cells (e.g., macrophages (MPs)) of the intestine.[10] Furthermore, increased CD98 expression has been found in colonic tissues from mice with active colitis[11] and in colonic biopsies from patients with Crohn's disease.[9] As CD98 expression plays crucial roles in controlling homeostatic and innate immune responses in the gut, the modulation of CD98 expression in colonic cells (epithelial and nonepithelial cells) could be a promising strategy for the treatment and prevention of inflammatory intestinal diseases, such as IBD.

To achieve a local downregulation of inflammation, small-interfering RNA (siRNA)-mediated knockdown of specific protein expression at the messenger RNA (mRNA) level[12] is an attractive therapeutic strategy. One of the major obstacles limiting the use of siRNA therapy has been the low penetration of naked siRNA across cell membranes.[13] Several delivery systems have been investigated to overcome this problem, and recent efforts in developing tissue-targeting nucleic acid delivery systems based on synthetic reagents have yielded promising results.[14–16] Among the drug carriers, nanoparticles (NPs; biodegradable or otherwise) have shown significant potential for binding and delivering siRNA.[17,18] Indeed, NPs have been shown to protect siRNAs against degradation *in vitro* and *in vivo*, and to markedly increase their pharmacological activities under both cell culture and physiological conditions.[16,18] In the context of IBD, a biocompatible system is needed. A previous study reported a biodegradable polymeric envelope that provides protection and transport of siRNA into the

Correspondence: *Hamed Laroui, Department of Chemistry and Biology, Center for Diagnostics and Therapeutics, Georgia State University, Atlanta, Georgia, USA. E-mail: hlaroui@gsu.edu*

cytosol, and facilitates efficient siRNA activity *in vivo*.[19] Here, we investigated the use of biodegradable, nontoxic NPs for targeting of CD98 siRNA, with the goal of inhibiting CD98 expression in colonic cells during intestinal inflammation.

We recently described an original technique for targeting the colon by loading the anti-inflammatory peptide, KPV, into NPs and encapsulating them in an alginate-chitosan hydrogel, thereby forming "hierarchical nano-micro particles." We found that daily gavage of KPV-loaded encapsulated NPs during dextran sodium sulfate (DSS) treatment offered a versatile drug delivery system. It was able to overcome physiological barriers and target KPV to inflamed colonic regions at a 1,200-fold lower concentration compared with KPV given in free solution, with a similar therapeutic efficacy. In the present study, we tested the therapeutic effect of hierarchical nano-micro particles loaded with "molecularly specific" CD98 siRNA, in terms of their abilities to target colonic cells and decrease colitis.

RESULTS

Characterization of NPs

Polylactic acid (PLA) NPs loaded with CD98 siRNA/polyethyleneimine (PEI) (**Figure 1a**) were synthesized as described in our previous study.[18] As shown in **Figure 1b**, scattering electron microscopy demonstrated that NPs made of PLA covered with polyvinyl alcohol (PVA) and loaded with CD98 siRNA/PEI complexes had a homogenous size distribution (~450 nm). Particle size and distribution were also checked by atomic force microscopy (AFM), which requires fewer preparatory steps than scattering electron microscopy and yields a direct picture. As shown in **Figure 1c**, AFM confirmed the size as ~450 nm and identified the distribution as unimodal. Finally, direct light-scattering measurement (based on photon correlation spectroscopy) confirmed the diameter of the NPs as 480 nm (**Figure 1d**), and showed that they had a low index of polydispersity (I = 0.09). The surface charges (zeta potential of −5.26 mV) provided by the PVA surface layer allowed the NPs to be suspended in biological medium without forming aggregates.

PEI confers a high degree of complexation/protection for CD98 siRNA

In this section, we did not use the NPs. PEI is directly complexed with siRNA in order to demonstrate its protection against RNAse. Low molecular-weight PEI (<1 kDa) was used to condense the negatively charged CD98 siRNAs via the formation of electrostatic

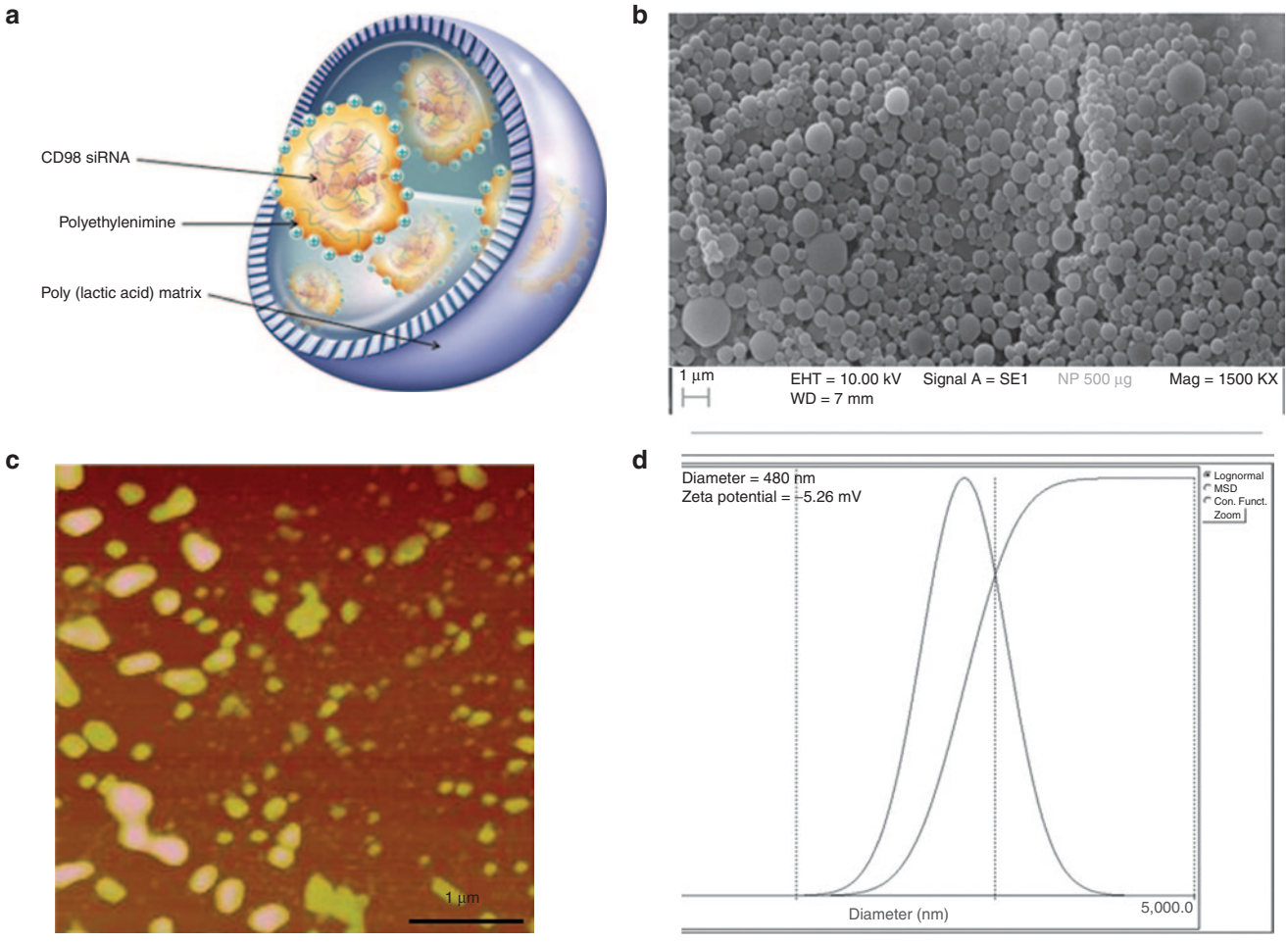

Figure 1 The physical and chemical properties of CD98 siRNA/PEI–loaded polylactic acid (PLA) nanoparticles (NPs). (**a**) Schematic structure of PLA NPs loaded with CD98 siRNA/PEI. (**b**) Scanning electronic microscopy of CD98 siRNA/PEI–loaded NPs (500 µg/ml in suspension). (**c**) Atomic force microscopy of CD98 siRNA/PEI–loaded NPs (500 µg/ml in suspension, scale bar is 1 µm). (**d**) Size distribution and zeta potential (mV) measured by light-scattering analysis.

interactions. The N/P ratio, which represents the ratio between the number of negative charges on the siRNA (P is the negative phosphorous charge) and the positive charges of the PEI (N is the positive ammonium charge), was calculated. The N/P ratio was optimized and set at 30 for PEI, as previously described.[18] To investigate PEI-mediated siRNA complexation/protection, we performed electrophoretic migration on a 4% agarose gel for 45 minutes at 100 V. As shown in **Figure 2a**, compared with the size marker (**Figure 2a**, lane 4), the free CD98 siRNA showed a band at 21 bp (**Figure 2a**, lane 2). In contrast, the PEI-complexed form was observed as a bright band in the loading well, showing that CD98 siRNA was strongly associated with PEI at the analyzed N/P ratio (and thus was too large to migrate inside the gel) (**Figure 2a**, lane 1). Furthermore, the PEI-complexed CD98 siRNA was not degraded by incubation with RNase A (0.04 mg/ml) at 37 °C for 1 hour. The band brightness of complexed siRNA (**Figure 2a**, lane 1) was slightly lower than the same amount of noncomplexed siRNA (**Figure 2a**, lane 2) because of the ability of PEI to quench siRNA/ethidium bromide fluorescence.[20] We also have previously demonstrated that siRNA/PEI complexation increased the rate of encapsulation of siRNA inside the NPs.[18]

PVA-covered, CD98 siRNA/PEI–loaded NPs do not affect cell viability

PEI is a common transfection agent that has been shown to efficiently deliver oligonucleotides (e.g., siRNA, plasmids, etc.) into cells.[18,21,22] The properties of PEI are strongly correlated with the molecular weight of the polymer. In general, low molecular-weight PEI (<1 kDa) is biocompatible and nontoxic[23] but has a low efficiency of transfection, whereas the same concentration (within a certain range) of high-molecular-weight PEI (>1,000 kDa) is biocompatible and has a high transfection efficiency, but shows cytotoxicity. Our strategy was to load low molecular-weight PEI on the NPs, in an effort to efficiently deliver siRNA while avoiding cytotoxicity. To verify this strategy, we used various concentrations (0–200 µg/ml) of NPs loaded with or without PEI for WST-1 cytotoxicity tests on mouse MPs (RAW 264.7 cells) for 48 hours. As shown in **Figure 2b**, both types of NPs (loaded or not with PEI) had no apparent cytotoxic effect on RAW 264.7 cells. Thus, we were able to target more PEI/siRNA complexes using NPs compared with systems that use naked PEI/siRNA complexes during transfection assay.[18]

PVA-covered CD98 siRNA/PEI–loaded NPs do not affect the epithelial barrier

Electric cell substrate impedance sensing (ECIS) is commonly used in our laboratory to study the resistance of epithelial cells, such as HT-29-19A or Caco2-BBE cells[24,25] and test the biocompatibility of molecules or nanosystems with epithelial cells (e.g., Caco2-BBE cells). In ECIS, a monolayer of epithelial cells with tight junctions creates a resistance that reaches a plateau when cells are fully differentiated and confluent. Treatment with a toxic molecule decreases the monolayer resistance. Here, we tested

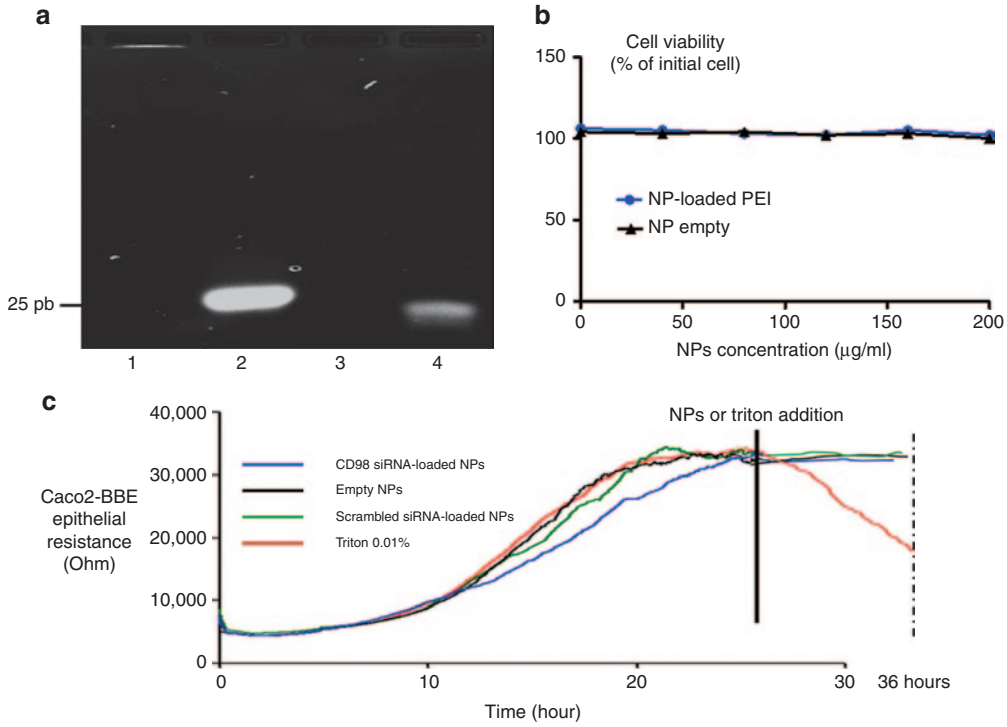

Figure 2 Polyethyleneimine (PEI) complexation, protection of CD98 siRNA against RNase A, and cytotoxicity of PEI in mouse macrophages (Raw 264.7) and epithelial cells (Caco2-BBE). (**a**) Electrophoretic migration in a 4% agarose gel containing 0.4 µg/ml (w/v) of (1) complexes formed of PEI and CD98 siRNA and supplemented with RNase A for 1 hour, (2) free CD98 siRNA, (3) free CD98 siRNA digested with RNase A for 1 hour, and (4) size marker (25 bp). (**b**) Cytotoxicity of various concentrations of nanoparticles (NPs) loaded (NP-loaded PEI) or not (NP empty) with PEI in Raw 264.7 cells after a 48-hour incubation. (**c**) CD98 siRNA/PEI–loaded polylactic acid (PLA) nanoparticles (NPs) do not affect the barrier function of Caco2-BBE cells. Epithelial barrier resistance (Ohms) of Caco2-BBE cells before and after addition of CD98 siRNA/PEI-loaded PLA NPs (1 mg/ml, blue line), 0.01% Triton (red line), scrambled siRNA-loaded NPs (1 mg/ml, green line), and empty NPs (1 mg/ml, black line).

intestinal monolayers with 1 mg/ml of CD98 siRNA/PEI–loaded NPs, 0.01% Triton (positive control), empty NPs, and scrambled siRNA-loaded NPs. As shown in **Figure 2c**, the addition of CD98 siRNA/PEI–loaded NPs did not significantly alter cell resistance compared with the pretreatment value (33.5 kΩ versus 35 kΩ, respectively after 24 hours). The positive control (0.01% Triton) dramatically decreased the epithelial resistance to 5 kΩ, whereas the empty or scrambled siRNA-containing NPs had no cytotoxic effect on the epithelial monolayers. These results indicate that NPs and most interestingly CD98 siRNA/PEI–loaded NPs are biocompatible with and not toxic to IECs.

FITC-tagged siRNA/PEI-loaded NPs covered with PVA are rapidly taken up by murine MPs (Raw 264.7)

Next, we have investigated the siRNA/PEI-loaded NPs uptake by MPs cells. The actin cytoskeleton and nucleus were stained using rhodamine phalloidin (red) and DAPI (purple), respectively. As shown in **Figure 3a**, cellular uptake differed significantly between Lipofectamine-mediated transfection of fluorescein isothiocyanate (FITC)-tagged siRNA (green) and treatment with PVA-covered siRNA-loaded NPs (200 µg/ml). NPs were effectively taken up by Raw 264.7 cells after 1 hour of exposure (**Figure 3b**). Intracellular loading of these molecules was maximal at 1 hour after NP addition, as no further increase in the fluorescence signal was observed thereafter (data not shown). In contrast, a weak fluorescence signal was observed beginning 2 hours after we used Lipofectamine to transfect cells with the same amount of free FITC-tagged siRNA (**Figure 3a**). Furthermore, Lipofectamine-treated Raw 264.7 cells formed dendrites, reflecting that Lipofectamine causes low-level inflammation in MPs.[18] In contrast, PEI loaded in NPs did not have any toxic effect on Raw 264.7 cells (**Figure 3b**), consistent with previous studies on PEI-mediated transfection of siRNA or plasmids.[18,26]

As the two-dimensional fluorescent pictures of MPs exposed to FITC-tagged siRNA NPs were not sufficient to demonstrate

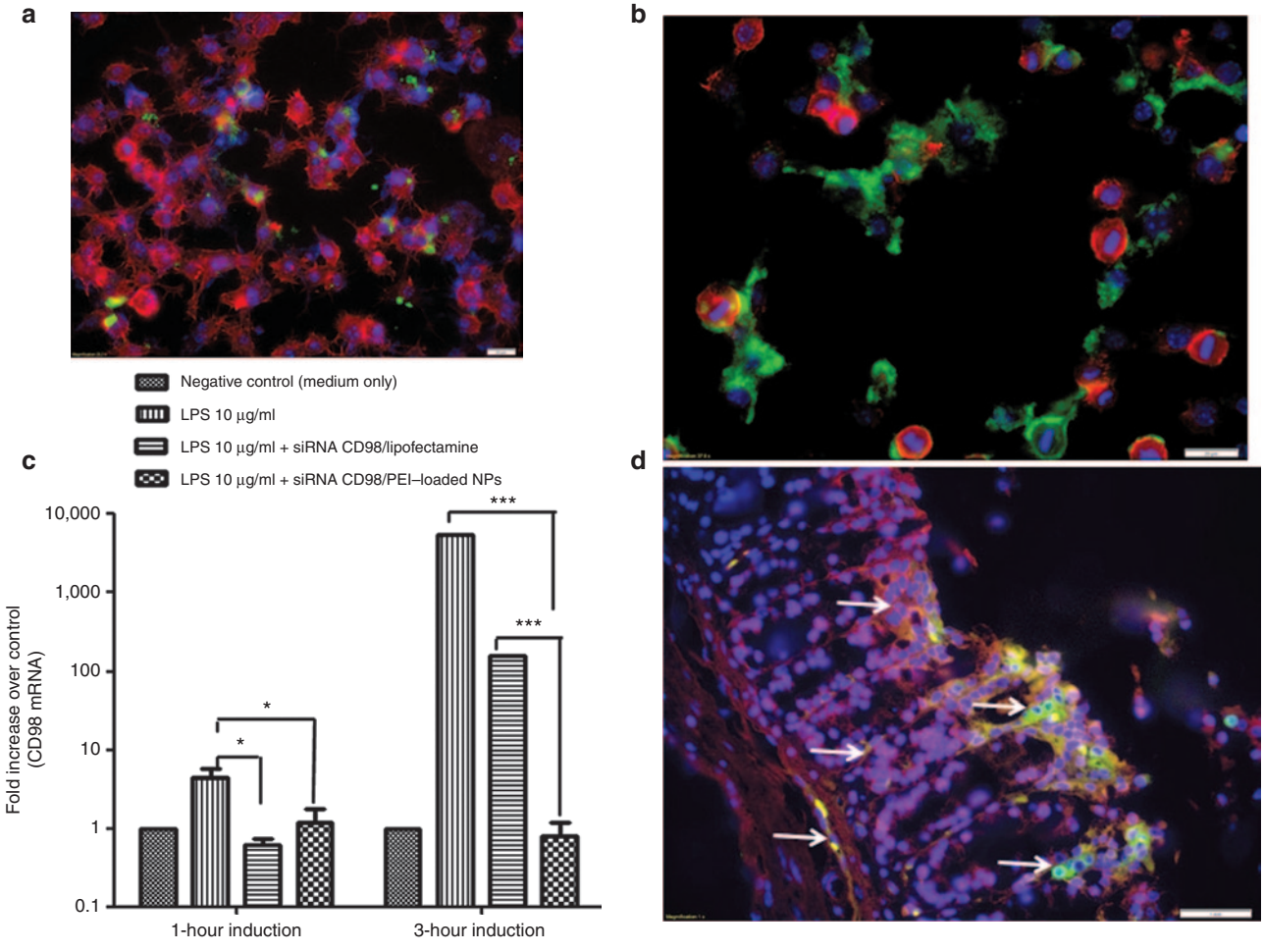

Figure 3 FITC-tagged polyvinyl alcohol (PVA)-covered siRNA/polyethyleneimine (PEI)-loaded nanoparticles (NPs) are rapidly taken up by murine macrophages (Raw 264.7 cells) and epithelial cells (total colon explants), and the CD98 siRNA is successfully delivered to the cytosol. (**a**) Fluorescent microcopy of Raw 264.7 cells (nucleus in purple and cytosol in red) that underwent Lipofectamine-mediated transfection with FITC-tagged siRNA (green) for 1 hour. (**b**) Fluorescent microcopy of FITC-tagged siRNA/PEI-loaded NPs (green) (200 µg/ml) taken up by Raw 264.7 cells (nucleus in purple and cytosol in red) after 1 hour of incubation. (**c**) Downregulation of CD98 mRNA in Raw 264.7 cells stimulated for 1 or 3 hours with lipopolysaccharide (LPS) after overnight pretreatment with CD98 siRNA–loaded NPs (siCD98-NPs), empty NPs (positive control), and Lipofectamine-delivered CD98 siRNAs. The control represents nonstimulated Raw 264.7 cells. (**d**) Uptake of FITC-tagged siRNA-loaded NPs (0.5 mg/ml) in contact for 6 hours with a total mice colon explant in RPMI medium. Tissues were fixed in buffered formalin (10%) and stain for F-actin (Alexa Fluor 568 phalloidin, red) and nucleus (DAPI, purple). Arrows indicate FITC signal of NPs (green).

the endocytosis of NPs into cells, we used a confocal strategy to obtain three-dimensional pictures. Using the *z*-stack approach, we "sliced" MPs that had been exposed to FITC-tagged siRNA-loaded NPs. We used a slicing increment of 1 µm; the first picture (z = 0 µm) was taken at the bottom of the cell, while the last one (z = 8 µm) was taken at the top of the cell. As shown in **Supplementary Figure S1**, a significant NP-associated FITC signal (green) was present in every slice of the NP-treated cell, visible in the cytosolic compartment between the nucleus (purple) and the cell membrane (red). This clearly shows that NPs were not retained at the surface of MPs, but rather were brought into the cytoplasm. These findings collectively demonstrated that our NPs are efficient vehicles that are capable of protecting siRNAs from the hostile extracellular environment and rapidly delivering them into the cytoplasm.

CD98 siRNA/PEI–loaded NPs efficiently deliver siRNA to MPs RAW 264.7 cells

Although our experiments confirmed that FITC-tagged siRNA/PEI is released in the cytosol of Raw 264.7 cells, we wanted to ensure the effectiveness of the CD98 siRNAs in our system. Thus, we next assessed the downregulation of CD98 expression by siRNA-loaded NPs *in vitro* in Raw 264.7 cells stimulated with 10 µg/ml lipopolysaccharide (LPS) for 1 and 3 hours. Raw 264.7 cells were exposed to CD98 siRNA/PEI–loaded NPs (~0.167 µg/mg) or the same amount of CD98 siRNA complexed with Lipofectamine for 24 hours, followed by stimulation with 10 µg/ml LPS. All cells showed similar levels of LPS-mediated stimulation (data not shown). LPS treatment increased the mRNA expression of mouse CD98 in Raw 264.7 cells by 50- and 5,275-fold after 1 and 3 hours of induction, respectively (**Figure 3c**), whereas CD98 siRNA/PEI–loaded NPs and CD98 siRNA/Lipofectamine significantly decreased this induction of CD98 expression. CD98 siRNA/PEI–loaded NPs decreased CD98 mRNA expression by fivefold after 1 hour of LPS induction (compared with the positive control at 1 hour) and by 2,600-fold after 3 hours (**Figure 3c**). CD98 siRNA/Lipofectamine, in contrast, only decreased CD98 expression by 33-fold after 3 hours (**Figure 3c**). Thus, after 3 hours of LPS induction, our NPs were 100 times more effective than Lipofectamine (which was applied at a higher dose than the NPs). These findings confirm the results from our fluorescent microcopy of FITC-siRNA–loaded NPs (**Figure 3a,b**). Together, these biological effects show that the high uptake of NPs into cells effectively downregulates CD98 mRNA expression in Raw 264.7 MPs, indirectly demonstrating that the CD98 siRNAs are released from endocytic vesicles. This is consistent with previous reports that PEI-based delivery systems have strong buffer capacities, yet do not require endosome-disrupting agents for lysosomal escape.[27]

FITC-tagged siRNA/PEI-loaded NPs covered with PVA are rapidly taken up by epithelial cells from colon explants of mice

Next, we have investigated the siRNA/PEI-loaded NPs uptake by epithelial cells from colon explants of mice. Once the NPs released from the hydrogel, NPs has to go through the mucus layer of the colonic epithelial cells. Using colon explants from healthy mice (with the maximal thickness and the maximal barrier function of the mucus), we showed that NPs (0.5 mg/ml) had the capability to evade the sub mucosal epithelium (indicated by arrows in **Figure 3d**). **Figure 3d** confirmed that after the release of NPs by the hydrogel in the colon, the NPs will be able to rapidly interact with local mice epithelial cells. Thus, we showed that siRNA-loaded NPs can successfully pass the mucus layer of the colon and be uptaken by epithelial cells.

Encapsulated CD98 siRNA/PEI–loaded NPs inhibit DSS-induced colonic inflammation in mice

Next, we investigated the effect of daily oral administration of encapsulated CD98 siRNA/PEI–loaded NPs on DSS-induced colitis in mice. To deliver the CD98 siRNA/PEI–loaded NPs to the colonic lumen, we encapsulated them in a biomaterial comprising alginate and chitosan at a ratio of 7/3 (wt/wt). We gavaged the mice each days of the induction of colitis by DSS (8 days), with the hydrogel-encapsulated NPs (5 mg/ml). We previously showed that this biomaterial collapses in intestinal solutions at pH 5 or 6, which are the colonic pH values seen under inflamed and noninflamed states, respectively.[28] Thus, the hydrogel releases the NPs preferentially in the colonic lumen versus other parts of the gastrointestinal tract, such as the stomach and small intestine.[28] The alginate/chitosan material was produced as previously described,[18,28] loaded with NPs (5 mg/ml), and chelated with calcium and sulfate ions to form a hydrogel of polysaccharide-encapsulated NPs. Scattering electron microscopy (**Figure 4a**) showed that NPs were successfully encapsulated in the hydrogel, with the polymer network forming small pores. This network is very stable at low pH and prevents the NPs from being released too early.[28] Once the hydrogel reaches the colon (*i.e.*, pH 5 or 6), the pores of polysaccharides chains network enlarge, allowing the NPs to escape.

Prior to analyzing the biological effects of CD98 siRNA/PEI–loaded NPs on DSS-induced colitis, we assessed safety parameters by analyzing the potential systemic dissemination of lactic acid (a degradation product of our NP formulation). Reverse-phase high performance chromatography (RP-HPLC) was used to quantify lactic acid in serum samples from mice treated with or without NPs. As shown in **Supplementary Figure S2**, the integrated peak areas did not significantly differ between NP-treated (36.3 mAU.s) and untreated (35.9 mAU.s) mice, indicating that there was no detectable dissemination of NP degradation products in the sera of NP-treated mice. As a positive control for the RP-HPLC, we supplemented the serum of an untreated mouse with 30, 60, 210, and 300 µl of lactic acid (2.4 mg/ml), and confirmed the accuracy of peak selection by showing that the peak localized at 2.4 minutes increased proportionally with the added lactic acid (table in **Supplementary Figure S2**).

In studies using the 3% DSS-induced mouse model of colitis, weight loss is typically used as a main marker of the colitis phenotype. In control mice that received DSS alone, weight loss reached 10% after 8 days of DSS treatment (**Figure 4b**). Mice treated with DSS and hydrogel containing empty NPs showed a similar 10% loss of initial body weight, indicating that the empty NPs did not attenuate the DSS-induced colitis. In contrast, mice gavaged with hydrogel containing the CD98 siRNA/PEI–loaded NPs lost only 3% of their initial body weight, which was a significant

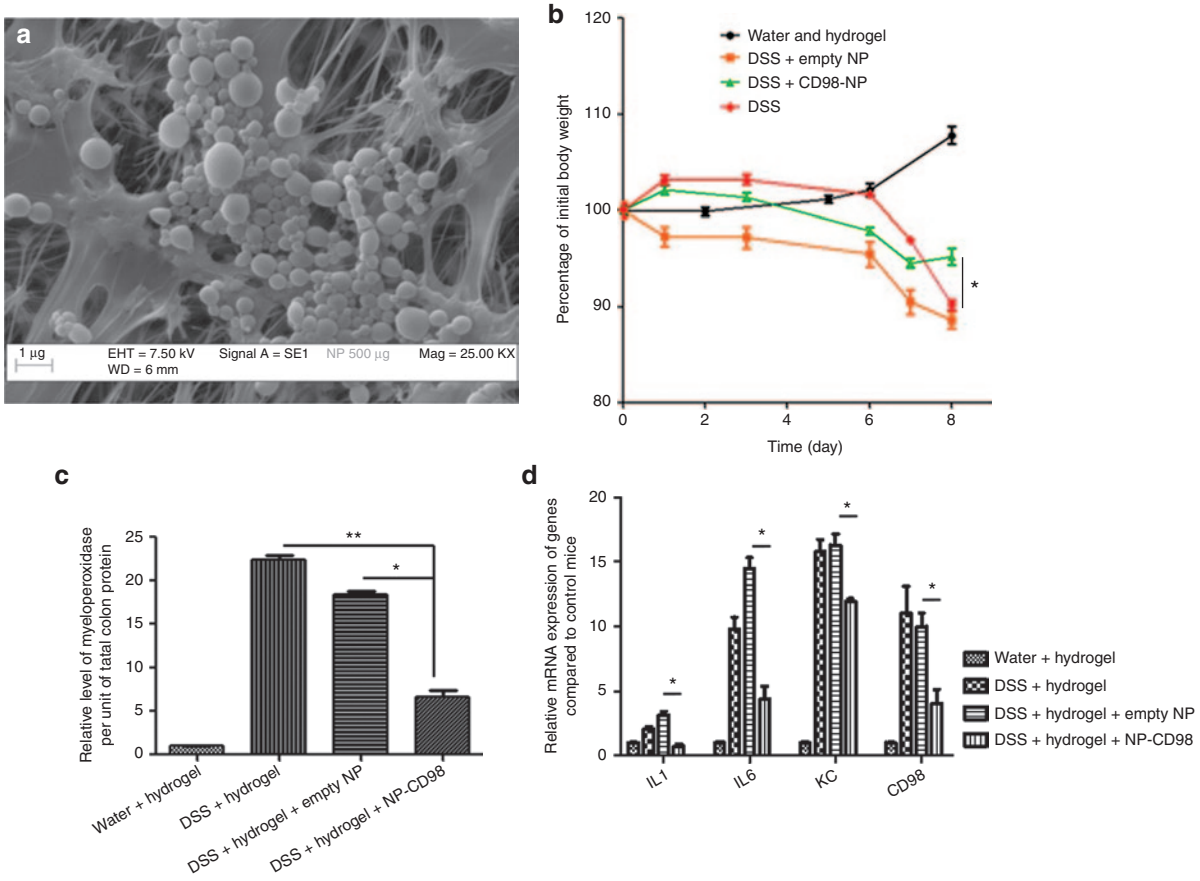

Figure 4 Daily gavage of hydrogel-encapsulated CD98 siRNA/polyethyleneimine (PEI)–loaded polylactic acid (PLA) nanoparticles (NPs) reduces inflammation in 3% dextran sodium sulfate (DSS)-treated mice. (**a**) Scanning electronic microscopy of CD98 siRNA/PEI–loaded NPs (500 µg/ml suspension in alginate/chitosan hydrogel). (**b**) Percentage of initial weight loss by water-control mice (water and hydrogel), and DSS-treated mice gavaged with empty NPs (DSS + empty NP), CD98 siRNA/PEI–loaded NPs (DSS + CD98-NP) or without NPs. (**c**) Myeloperoxidase (MPO) levels in colon samples from water-control mice (water + hydrogel), and DSS-treated mice gavaged with empty NPs, CD98 siRNA/PEI–loaded NPs, or without NPs (DSS + hydrogel). (**d**) The mRNA expression levels of CD98 and major proinflammatory cytokines and chemokines (IL-1β, IL-6, and KC) in the various groups of DSS-treated mice.

improvement over the DSS-treated group (**Figure 4b**). We also measured myeloperoxidase (MPO) activity, which is a direct indicator of neutrophil infiltration into the colonic mucosa, and thus an important marker of inflammation during DSS treatment.[29] As shown in **Figure 4c**, MPO levels confirmed that inflammation was attenuated in mice gavaged with hydrogel containing CD98 siRNA/PEI–loaded NPs (DSS+hydrogel+NP CD98). DSS-treated mice (DSS+hydrogel) showed fourfold less MPO activity in the colon compared with DSS-treated mice gavaged with empty NPs (DSS+hydrogel+empty NP; **Figure 4c**). We also used qPCR to measure the mRNA levels of CD98 and proinflammatory cytokines (interleukin 1β (IL-1β), IL-6, and keratinocyte chemoattractant (KC)) in colon tissues during DSS-induced colitis. CD98 mRNA expression was reduced by threefold in mice that received DSS+hydrogel+NP CD98, compared with mice treated with DSS alone or DSS and empty NPs, while IL-1β, IL-6, and KC were reduced by 50%, 33% and 50%, respectively in DSS+hydrogel+NP CD98–treated mice compared with the DSS-treated control (**Figure 4d**). Next, we analyzed cytokine secretion using a Meso Scale Discovery (MSD) cytokine assay on colon samples cultured from DSS-treated mice gavaged with hydrogel-encapsulated CD98 siRNA/PEI–loaded NPs (NP CD98), empty hydrogel-encapsulated NPs (NP empty) or hydrogel alone (DSS). Consistent with the results of our mRNA analyses, the expression levels of IL-1β, IL-6, and KC after DSS treatment were all reduced in NP CD98 mice (7-fold, 15-fold, and 5-fold, respectively) compared with NP empty or DSS mice (**Figure 5**).

To confirm our findings, histological analyses and colonoscopies were performed on water-control mice and DSS-treated mice gavaged with hydrogel containing empty NPs or CD98 siRNA/PEI–loaded NPs. As shown in **Figure 6a** (1,2), hematoxylin and eosin (H&E) staining showed normal physiology in water-treated colons, including normal crypt density, no distortion of the crypt architecture, a flat mucosal surface, and cellular infiltrates of normal density, distribution and population in the lamina propria. Colonoscopies of water-control mice showed that intact mucosa (white) protected epithelial cells from the external domain (**Figure 6c**, **3**). As shown in **Figure 6b** (1,2), the colons of DSS-treated mice were characteristic of the DSS-induced colitis model, with a disrupted epithelial architecture, nonflat mucosal surface, and significant infiltration of neutrophils into the lamina propria. Furthermore, colonoscopy revealed large ulcers, bloody stool, and complete disruption of the

mucosal layer (**Figure 6b**, **3**). Similar findings were obtained from mice treated with DSS and hydrogel containing empty NPs (data not shown). In contrast, mice treated with DSS plus hydrogel containing CD98 siRNA/PEI–loaded NPs showed significantly less inflammation; the overall architecture of the epithelial layer (crypts and villi) was maintained, and no blood bloody stool or exaggerated diarrhea was observed (**Figure 6c**, **1**–3). We finally quantified the severity of inflammatory infiltrate, extent of crypt damage and ulceration, and we generated a total histological score according to method previously used.[30] The histological score (**Figure 6a**–**c**, **4**) of the group treated with DSS and receiving empty NPs was significantly higher than the group treated with DSS and CD98 siRNA–loaded NPs (respectively 7.2 ± 0.7 versus 3.9 ± 0.6). Similarly, mice treated with CD98 siRNA–loaded NPs exhibited a lower total endoscopic score (**Figure 6a**–**c**, **5**). Thus, the histological score further confirmed the beneficial effect of the CD98 siRNA during DSS-induced colitis treatment. Together, these data show that treatment with our hydrogel-encapsulated CD98 siRNA/PEI–loaded NPs significantly reduced CD98 expression and overall inflammation in the DSS-induced mouse model of colitis.

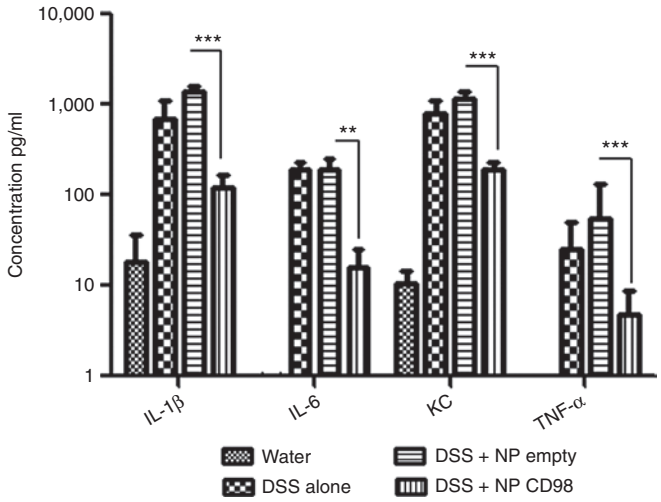

Figure 5 Daily gavage of CD98 siRNA/polyethyleneimine (PEI)–loaded polylactic acid (PLA) nanoparticles (NPs) reduces proinflammatory cytokines in DSS-treated mice. *Ex vivo* colonic concentrations of the cytokines and markers of inflammation: IL-1β, IL-6, KC, and TNF-α.

Encapsulated CD98 siRNA/PEI–loaded NPs are preferentially taken up by murine MPs and IECs compared with dendritic cells during DSS-induced colitis

We previously reported that our hydrogel-encapsulated NPs, given daily during DSS treatment, could specifically target the colon following ingestion via gavage.[18,28] Once the NPs are delivered to the colon, they interact with colonic cells *via* their external layer of PVA. To identify the colonic cell types that were able to take up the CD98 siRNA/PEI–loaded NPs in the present study, we obtained colon tissue samples from the various experimental groups and used multiple-color flow cytometer to sort cells according to the presence or absence of specific antibodies. We defined $CD45^+$MHC class $II^+CD11b^+Cd11c^-F4/80^+$ cells as MPs, $CD45^-$MHC Class II^- cells as IECs and $CD45^+$MHC class $II^+CD11b^+Cd11c^+F4/80^-$ cells as dendritic cells, and used a Alexa Fluor 647-conjugated CD98 to identify CD98-positive cells. We found that mice treated with DSS alone, DSS with hydrogel

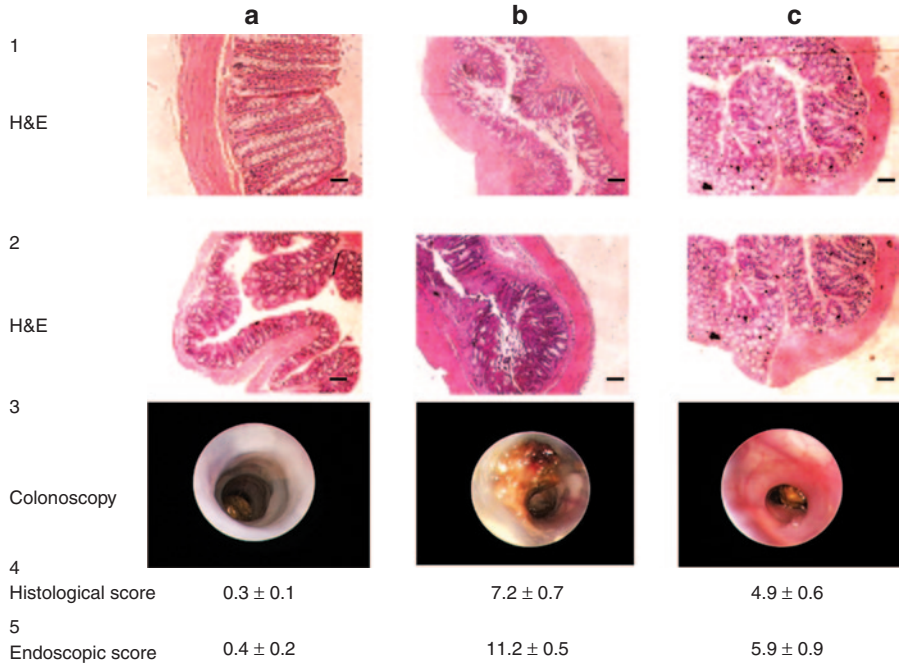

Figure 6 Daily gavage with CD98 siRNA/polyethyleneimine (PEI)–loaded polylactic acid (PLA) nanoparticles (NPs) reduces inflammation in dextran sodium sulfate (DSS)-treated mice. (1 and 2) H&E staining of colon sections from mice treated with (**a**) water, (**b**) 3% DSS + empty NPs, and (**c**) 3% DSS + CD98 siRNA/PEI NPs. (3) Colonoscopies of mice treated with (**a**) water, (**b**) 3% DSS + empty NPs, and (**c**) 3% DSS + CD98 siRNA/PEI NPs. Scale bar = 50 µm. (4) Histologic and (5) endoscopic score of severity of inflammatory infiltrate, extent of crypt damage and ulceration used to generate a total histological and endoscopic score.

containing empty NPs (empty NPs) or scrambled siRNA/PEI-loaded NPs, all had identical cell populations (**Figure 7a**). In **Figure 7b**, we noticed that DSS-induced colitis treatment increased CD98-positive in IECs and MPs when compared with untreated mice (97.0% of total IECs and 96.3% of total MPs for DSS-treated mice versus 63.8% of total IECs and 69.7% of total MPs for nontreated mice). In contrast, mice treated with DSS and hydrogel containing CD98 siRNA/PEI–loaded NPs had significantly fewer CD98-positive IECs and MPs when compared with DSS-treated mice (73.5% of total IECs and 60.4% of total MPs for mice treated with DSS and hydrogel containing CD98 siRNA/PEI–loaded NPs versus 97.0% of total IECs and 96.3% of total MPs for DSS-treated mice) (**Figure 7b**). Notably, these levels of CD98-positive cells were comparable with those observed in water-control mice (respectively 63.8% of total IECs and 69.7% of total MPs (**Figure 7a**,**b**). No significant change of CD98 expression was detected in dendritic cells from mice treated with DSS alone versus DSS plus hydrogel containing CD98 siRNA/PEI–loaded

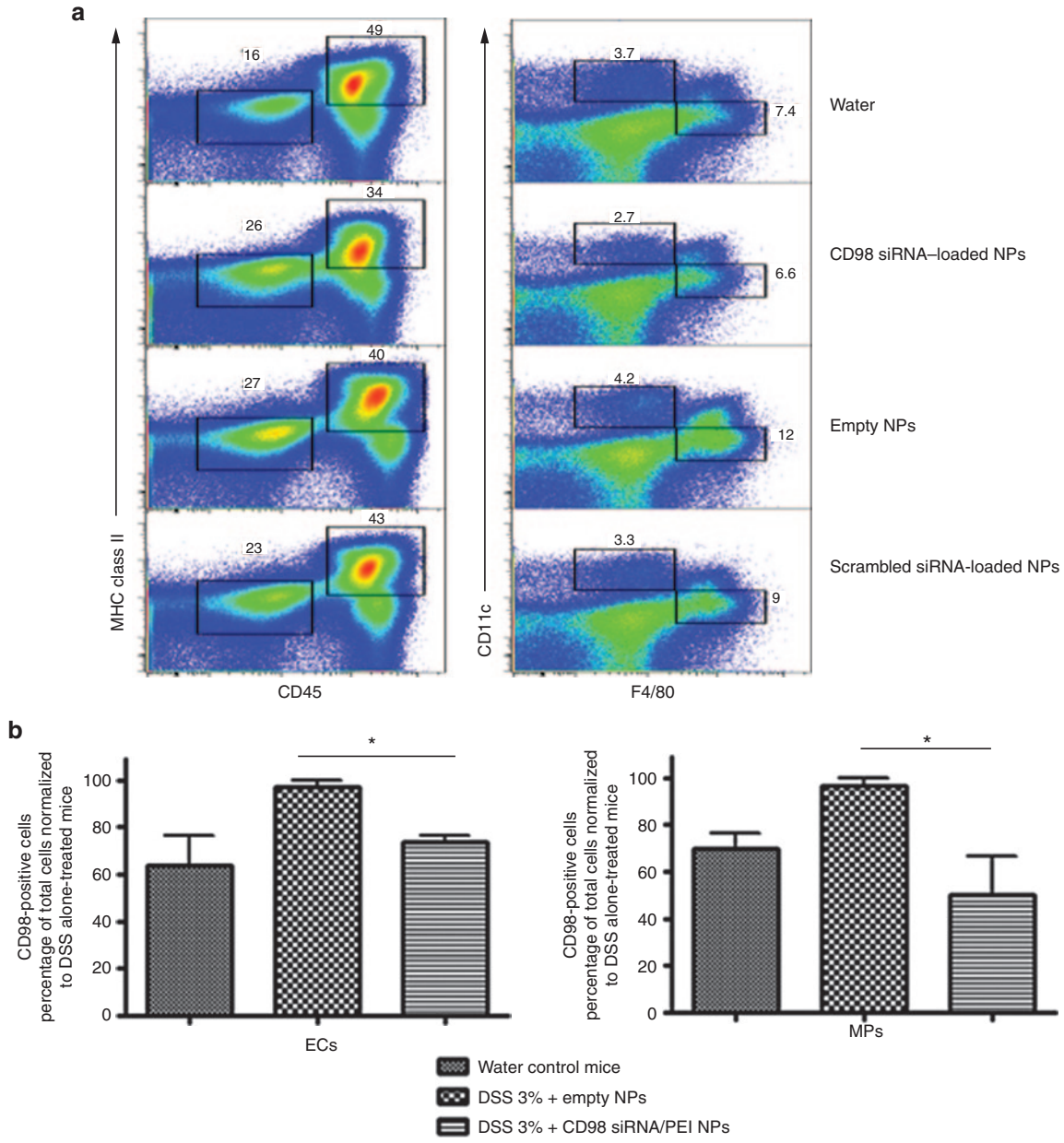

Figure 7 Flow cytometry analysis indicating that daily gavage of CD98 siRNA/polyethyleneimine (PEI)–loaded polylactic acid (PLA) nanoparticles (NPs) reduces CD98 expression mainly in macrophages (MPs) and epithelial cells of dextran sodium sulfate (DSS)-treated mice. (**a**) Representative FACS plots illustrating the gating strategy utilized to define dendritic cells (DCs), MPs, and intestinal epithelial cells (IECs) for DSS- and water (control)-treated mice that received daily gavages with CD98 siRNA/PEI–loaded NPs (CD98), BSA-loaded NPs (empty), and scrambled siRNA-loaded NPs (scramble). ECs were defined as $CD45^{-}$MHC Class II- and forward scatter low cells, MPs as $CD45^{+}$MHC class $II^{+}CD11b^{+}CD11c^{-}F4/80^{+}$ cells, and DCs as $CD45^{+}$MHC class $II^{+}CD11b^{+}CD11c^{+}F4/80^{-}$ cells. (**b**) Frequency of $CD98^{+}$ MPs and ECs of total cells for water (water-control mice) or DSS-treated mice receiving daily gavages with CD98 siRNA/PEI–loaded NPs (DSS 3% + CD98 siRNA/PEI–loaded NPs) or with BSA-loaded NPs (DSS 3% + empty NPs) normalized to DSS alone-treated group.

NPs. Together, these data indicate that PVA-covered NPs loaded with CD98 siRNA were mainly taken up by MPs and IECs, not by dendritic cells, in DSS-treated mice. We further used immunofluorescence microscopy to demonstrate that the NPs can interact with and be taken up by IECs and MPs. As shown in **Supplementary Figure S3**, we specifically stained colonic IECs (EpCAM+ cells, panel A) and colonic MPs (F4/80+ cells, panel B) in red, and used FITC-tagged siRNA-loaded NPs to assess colocalization (visualized as yellow spots; **Supplementary Figure S3**, arrows). We observed significant uptake of the FITC-tagged NPs by both colonic epithelial cells (crypt and surface) and colonic MPs. The results of this *ex vivo* experiment therefore indicate that the beneficial effects of our siRNA-loaded NPs are mediated by both colonic MPs and colonic epithelial cells.

DISCUSSION

Abnormal expression or function of CD98 and disruption of the interactions between CD98 and its binding partners can lead to defects in cell homeostasis and immune responses.[4] Indeed, increased CD98 expression levels in IECs and immune cells of the intestine have been correlated with disease conditions, such as inflammation and tumor metastasis.[4,31,32] We recently reported that CD98 expression in the colonic epithelium specifically regulates colonic micro RNA expression during intestinal inflammation.[33] Modulation of CD98 expression and/or function therefore represents a promising strategy for the treatment and prevention of IBD and colitis-associated cancer.

Most of the drugs used to treat these disorders become systemically bioavailable only at high dosages, and may trigger serious adverse effects.[31,34,35] Tumor necrosis factor α (TNF-α) plays a central role in the pathogenesis of IBD, and multiple clinical trials have shown that patients may be successfully treated with anti-TNF-α antibodies.[36,37] However, but nearly 25% of patients taking the monoclonal antibody, infliximab, experienced at least one serious adverse event, such as pneumonia, cancer, bacterial infection, or acute inflammation.[38–41] At present, the action mechanisms and exact target of these antibodies are not well understood. It is hoped, however, that strategies capable of targeting the inflamed intestine or disease site could allow the use of lower doses and reduce the adverse effects.[42]

Many diseases, including IBD and colitis-associated cancer, are caused by the inappropriate activity of various genes. The ability of siRNAs to specifically downregulate target genes thus provides an approach to treat a wide range of human diseases. In the present study, we used CD98-targeting siRNAs to specifically downregulate colonic CD98 expression, which has been implicated in colitis and colitis-associated cancer. To have the intended effects, however, the siRNAs must be appropriately and efficiently delivered. Here, we demonstrate that oral administration of hydrogel-encapsulated siRNA CD98/PEI–loaded NPs allowed low doses of siRNA CD98 to be specifically targeted to colonic epithelial and MPs cells, effectively reducing CD98 expression and decreasing colitis symptoms in a DSS-induced mouse model. We further demonstrate that CD98 controls (either directly or indirectly) the production of proinflammatory cytokines in this model. The link between colonic CD98 expression and cytokine production is not fully understood, but we recently showed that IEC-specific overexpression of CD98 results in intestinal barrier dysfunction, which is among the earliest events that precede evident inflammation, mucosal damage and spontaneous upregulation of proinflammatory genes in the DSS-induced mouse model of colitis. CD98 overexpression may also affect integrin signaling in IECs, disrupting the homeostatic regulation of cell proliferation and survival, potentially leading to an abnormal basal intestinal phenotype and contributing to increased intestinal permeability. Our analysis of cytokine gene expression does not provide direct mechanistic explanations; however, it highlights important differences in the inflammatory profiles of mice in which CD98 expression has been genetically manipulated. In the future, extensive characterizations of immune profiles could help elucidate the detailed mechanisms underlying CD98-mediated cytokine dysregulation. However, our present results suggest that targeted downregulation of CD98 expression in both epithelial cells and MPs could protect the intestinal barrier function and reduce MP activation.[10,43–45]

We herein demonstrate that we can deliver effective (yet low) doses of CD98 siRNA to mouse colonic epithelial cells and intestinal MPs via multiple oral administrations of encapsulated CD98 siRNA/PEI–loaded NPs. We found that the *in vivo* dose of encapsulated CD98 siRNA required to mediate gene silencing is 60 µg siRNA per kg, which is a respectively 10 to 40 times greater potency than previously reported in studies on local delivery in brain by microinfusion[46] or on systemic delivery by intravenous injection.[47] Our results demonstrate that CD98 siRNA is well protected by the NPs and its complexation to PEI, yet is able to escape lysosomes and be functionally present in the cell cytoplasm. In the future, it should be feasible to further reduce the required oral dose by increasing the stability and efficacy of CD98 siRNAs *via* chemical modifications, such as 2′MOE, FANA, 2′-Fluoro or LNA. Since there is a direct relationship between colonic CD98 expression and colitis/colitis-associated cancer, we are currently working to specifically target CD98 overexpressing colonic cells by using CD98 siRNA/PEI–loaded NPs coated with an anti-CD98 antibody.

In conclusion, we herein demonstrate the therapeutic effect of hierarchical nano-micro particles that home to the colon and directly release CD98-specific siRNAs to colonic cells, thereby decreasing colitis.

MATERIALS AND METHODS

Preparation of CD98 siRNA/PEI–loaded NPs covered with PVA. NPs were synthesized via double emulsion/solvent evaporation, as described previously.[28] Briefly, an internal phase (see details below) containing the drug was mixed with 20 g/l of polylactic acid (PLA) (Sigma, St Louis, MO) in dichloromethane to generate a water-in-oil (W/O) emulsion after 2 minutes of vortexing (Maxi Mix II, Thermodyne, Dubuque, IA) and 1 minutes of sonication with 50% active cycles at 70% power (P_{max} = 400 W) (Digital Sonifier 450, Branson, Danbury, CT). This first emulsion was dropped in a second water phase containing 0.3 g/l of PVA to generate a water/oil/water emulsion (W/O/W).

The W/O/W emulsion was dropped in a dispersing phase of 0.1 g/l PVA, and stirred at 45 °C under a vacuum to remove dichloromethane. NPs were centrifuged at 9,953*g* and freeze-dried overnight at −50 °C under 0.1 mbar pressure. As the second emulsion allowed PVA to be grafted on the surface by hydrophobic interaction with the PLA matrix, NPs were coated with PVA to prevent aggregations through electrostatic repulsions.

Preparation of the internal phase. The internal phase has a typical N/P ratio of the number of negative charges of siRNA (CD98 siRNA is a mix of 3 siRNAs as follows: sc-35034A, sc-35034B, and sc-35034C, Santa Cruz Biotechnology, Dallas, TX or FITC-CD98 siRNA) (P as the phosphorous charge) and positive charges of PEI (N as the ammonium charge) (N/P ratios of 30 for PEI). A mixture of siRNA/PEI: 29 µl CD98 siRNA (5 µmol/l) was combined with 18 µl PEI (5 mmol/l), and incubated for 10 minutes at room temperature for complexation. After 10 minutes, a polyplex was formed, and 750 µl bovine serum albumin (BSA, 50 g/l) added, generating the first emulsion with dichloromethane.

Scattering electron microscopy. NPs specimens were applied to glass coverslips, air dried and sputter coated with Au/Pd using a Denton desktop sputter coater (Moorestown, NJ). The microscope used to take the picture was a LEO 1450VP (New York, NY).

AFM measurement. For AFM test, a drop of NPs made of PLA suspension was deposited onto a freshly cleaved mica slide, followed by drying overnight at 25 °C. The images were taken using a SPA 400 AFM (Seiko instruments, Chiba, Japan) at tapping mode using high resonant frequency (F0 = 150 kHz) pyramidal cantilevers with silicon probes at a scan frequency of 1 Hz.

NPs size and zeta potential measurements. Diameters (nm) and zeta potential (mV) of NPs were measured by light scattering using 90 Plus/BI-MAS (multi-angle particle sizing) or light scattering after applying an electric field using a ZetaPlus (zeta potential analyzer, Brookhaven Instruments, Holtsville, NY). The average and standard deviations of the diameters (nm) or zeta potential (mV) were calculated using three runs. Each run was an average of 10 measurements.

CD98 siRNA/PEI polyplex formation and protection from RNAse A. Formation of each polyplex was assessed via examination of electrophoretic mobility on a 4% (w/v) agarose gel for 45 minutes at 100 V in 0.5X TBE buffer (40 mmol/l Tris/HCl, 445 mmol/l boric acid, and 1 mmol/l ETDA). Ethidium bromide was used to stain siRNA.

The polyplex was incubated with 4 µl of RNase A (0.04 mg/ml) at 37 °C for 1 hour. Polyplex and siRNA integrity were assessed via electrophoretic mobility analysis.

Cell culture. RAW 264.7 cells (MPs) were cultured to confluence in 75-cm^2 flasks at 37 °C in a humidified atmosphere containing 5% (v/v) CO_2. The culture medium was DMEM/Ham's F-12 medium (Invitrogen, Grand Island, NY) supplemented with l-glutamine (2 mm), penicillin (100 units/ml), streptomycin (100 µg/ml), and heat-inactivated fetal calf serum (10%, v/v) (Atlanta Biologicals, Atlanta, GA). For the fluorescent study, we placed a plate checker in the incubator (15 minutes, 200 Hz).

WST-1. To assess the potential toxicity of empty and CD98 siRNA/PEI–loaded NPs, a WST-1 assay was performed. As described previously,[48] RAW 264.7 cells were seeded in 96-well plates at a density of 5×10^4 cells per well and exposed to 1 mg/ml of empty NPs (dark line) and NPs loaded with CD98 siRNA/PEI (blue line) for 48 hours. The WST-1 assay measures cleavage of the soluble red tetrazolium salt, WST-1 (4-[3-(4-iodophenyl)-2-(4-nitrophenyl)-2H-5-tetrazolio]-1,3-benzene disulfonate), by dehydrogenase present in intact mitochondria, which leads to the formation of dark red formazan crystals. WST-1 proliferation reagent (10 µl) was added to cells (10 µl/well) and incubated for 1–2 h at 37 °C. The wavelength for measuring absorbance of the formazan product was 440 nm.

Electric cell substrate impedance sensing. For experiments using the ECIS (Applied BioPhysics, Troy, NY) system, ECIS 8W1E arrays were used (Applied BioPhysics). As previously described,[24] Caco2-BBE cells were plated at 4×10^5 cells per well and experiments were performed 3 days after seeding when cells are at confluency. At confluency, suspensions of 1 mg/ml of the studied NPs were added and the variation of resistance was measured in real time.

Intracellular NP uptake visualization. Confocal microscopy was employed to visualize the intracellular uptake of NPs (Zeiss LSM510 Meta Confocal). Cells (10^4) were seeded in four-chamber tissue culture glass slides (BD Falcon, Bedford, MA). For siRNA uptake, MPs (200 µg/ml) were exposed to FITC siRNA–loaded NPs for 1 hour or with FITC siRNA transfected by lipofectamine. Next, MPs were washed three times with medium and three times with phosphate-buffered saline to remove extracellular NPs, and subsequently fixed for 20 minutes in 4% paraformaldehyde. Alexa Fluor 568 phalloidin and DAPI were successively added, and diluted 60 and 10,000 times for staining cells for 45 minutes and 5 minutes, respectively. To obtain comparable data, all photomultipliers used were adjusted to the same sensitivity (gain/offset).

Ex vivo *colon culture for FITC-tagged siRNA-loaded NPs uptake by epithelial cell from murine colon explants.* For *ex vivo* colon culture, mice of 8 weeks old were killed. Colons were harvested and cut longitudinally to be placed in a petri dish containing RPMI medium (Corning, Manassas, VA) supplemented with 10% fetal bovine serum, and 1.5 µg/ml plasmocin (Invitrogen).

Tissues were then exposed to 0.5 mg/ml of FITC siRNA–loaded NPs for 6 hours. Tissues were then rinsed three times in phosphate-buffered saline and fixed in 10% formalin and stained with Alexa Fluor 568 phalloidin (F-actin) and DAPI (nucleus) successively added and diluted 60 and 10,000 times for staining cells for 45 minutes and 5 minutes, respectively. To obtain comparable data, all photomultipliers used were adjusted to the same sensitivity (gain/offset).

DSS-induced colitis. Colitis was induced by 3% (w/v) DSS (molecular weight 42 kDa; ICN Biochemicals, Aurora, OH) added to the drinking water. Colonic inflammation was assessed 8 days after DSS treatment. Eight mice were included in each group.

Gavage of scrambled and CD98 siRNA/PEI–loaded NPs encapsulated in hydrogel. Chitosan powder was solubilized in acetic acid then neutralized by addition of NaOH (0.1 mol/l) to give a final chitosan concentration of 0.6% (wt/vol). Medium-viscosity sodium alginate was prepared in NaCl (0.15 mol/l) 1.4% (wt/vol). Before mixing with NaCl, or acetic acid, the polymer powders were weighed, placed in glass tubes, and autoclaved. Alginate solution and chitosan solutions were mixed at a 1:1 ratio for a final concentration of 7 and 3 g/l, respectively. The polymer suspension was homogenized for 24 hours.

Different NPs were added to obtain 5 mg/ml concentration of hydrogel solution and stirred to disperse NPs throughout the polymer solution. A chelation solution containing 70 mmol/l of calcium chloride and 30 mmol/l of sodium sulfate was prepared. Procedure for inclusion of loaded NPs into biomaterials and the gavage method are available at http://www.natureprotocols.com/2009/09/03/a_method_to_target_bioactive_c.php.

C57BL/6 mice (8 per group) were receiving daily gavages during the 8 days of DSS treatment with encapsulated CD98 siRNA/PEI–loaded, scramble siRNA-loaded, or empty NPs. Then, mice were killed and colons were collected for biological analysis.

MPO assay. Colonic tissue samples were homogenized in ice-cold potassium phosphate buffer (50 mmol/l K_2HPO_4 and 50 mmol/l KH_2PO_4, pH 6.0) containing 0.5% hexadecyltrimethylammonium bromide (Sigma-Aldrich, St Louis, MO). The homogenates then were sonicated, freeze-thawed three times, and centrifuged at 17,500 relative centrifugal force for 15 minutes. Supernatants (20 µl) or MPO standard were added to 1 mg/ml o-dianisidine hydrochloride (Sigma-Aldrich) and 0.0005% H_2O_2, and the change in absorbance at 450 nm was measured. One unit of MPO activity was defined as the amount that degraded 1 µmol peroxidase per minute. The results were expressed as absorbance per microgram of protein.

RT-PCR and qRT-PCR. Total RNA extracted using TRIzol (Invitrogen) or RNeasy Mini Kit (Qiagen) was reverse transcribed using the First Strand

cDNA Synthesis Kit (Fermentas). RT-PCR was performed using the GeneJET Fast PCR kit (Fermentas). qRT-PCR was performed using SYBR Green qPCR Master Mix (Fermentas) on a Mastercycler Realplex4 (Eppendorf). 36B4 was used as housekeeping gene. Fold-induction was calculated using the Ct method: $\Delta\Delta Ct = (Ct_{Target\ gene} - Ct_{housekeeping\ gene})_{treatment} - (Ct_{Target\ gene} - Ct_{housekeeping\ gene})_{nontreatment}$, and the final data were derived from $2^{-\Delta\Delta Ct}$.

Primers used for RT-PCR and qRT-PCR: mouse CD98 for: 5′-GAGGACAGGCTTTTGATTGC-3′, mouse CD98 rev: 5′-ATTCAGTA CGCTCCCCAGTG-3′, KC for: 5′-TTGTGCGAAAAGAAGTGCAG-3′, KC rev: 5′-TACAAACACAGCCTCCCACA-3′, IL-1β for: 5′-TCGC TCAGGGTCACAAGAAA-3′, IL-1β rev: 5′-CATCAGAGGCAAGGAGG AAAAC-3′, IL-6 for: 5′-ACAAGTCGGAGGCTTAATTACACAT-3′, IL-6 rev: 5′-TTGCCATTGCACAACTCTTTT C-3′. 36B4 was used as housekeeping genes. Fold-induction was calculated using the Ct method, $\Delta\Delta CT = (Ct_{Target}\text{-}Ct_{housekeeping})_{infected} - (Ct_{Target}\text{-}Ct_{housekeeping})_{uninfected}$, and the final data were derived from $2^{-\Delta\Delta CT}$.

Ex vivo *colon culture for measuring proinflammatory cytokines by Multiplex cytokine assays.* For *ex vivo* colon culture, mice of 8 weeks old were killed after 8 days of DSS (3%) treatment in drinking water. Four groups of mice were analyzed as followed: control mice (water) and mice receiving DSS alone (DSS alone), DSS with empty NPs (Empty NPs), and DSS with CD98 siRNA–loaded NPs (NP CD98). Colons were harvested and cut longitudinally to be placed overnight in a petri dish containing RPMI medium (Corning) supplemented with 10% fetal bovine serum, and 1.5 µg/ml plasmocin (Invitrogen). Supernatants were then collected and directly processed according to the multiplex cytokine assay protocol.

Multiplex cytokine assays. For the cytokines studies, the Mouse ProInflammatory 7-plex Ultra-sensitive kit from MSD (Gaithersburg, MD), which measures IL-6, KC, TNF-α, and IL-1β was used. Briefly, MSD provides a plate that has been precoated with capture antibody on spatially distinct spots antibodies for IL-1β, IL-6, KC, and TNF-α. The user adds the supernatant of *ex vivo* colon culture (see details in the same section) and a solution containing the labeled detection antibodies anti-IL-1β, anti-IL-6, anti-KC, and anti-TNF-α labeled with an electrochemiluminescent compound, MSD SULFO-TAG label. Analytes in the sample bind to capture antibodies immobilized on the working electrode surface; recruitment of the labeled detection antibodies by bound analytes completes the sandwich. After adding the MSD read buffer that provides the appropriate chemical environment for electrochemiluminescence, we loaded the plate into an MSD SECTOR instrument for analysis. Inside the SECTOR instrument, a voltage applied to the plate electrodes causes the labels bound to the electrode surface to emit light. The instrument measures intensity of emitted light to afford a quantitative measure of IL-1β, IL-6, KC, and TNF-α present in the sample. All standards and samples were measured in triplicate.

H&E staining. Colonic sections were fixed in 10% buffered formalin (EMD Millipore, Billerica, MA) and embedded in paraffin. 5-µm sections were stained with H&E. Photomicrographs were taken using an Olympus microscope and D-26 color camera at 20x magnification.

Endoscopic assessment of colitis. Direct visualization of DSS-induced colonic mucosal damage *in vivo* was performed using Coloview (Karl Storz Veterinary Endoscopy, Tuttlingen, Germany). Mice were supplied with food and water until the endoscopy was performed. Mice were anesthetized with 1.5%–2% isoflurane and 3 cm of the colon proximal to the anus was visualized after inflation of the colon with air. The endoscopic damage score was determined using a previously described scoring[30,49] method with one modification: assessment of colon translucency (0–3 points), presence of fibrin attached to the bowel wall (0–3 points), granular aspect of the mucosa (0–3 points), morphology of the vascular pattern (0–3 points), and stool characteristic (normal to diarrhea; 0–3 points) Since this scoring method did not include assessment for the presence of blood in the lumen, we added this parameter (0 points: no blood; 1 point: slight bleeding; 2 points: frank bleeding) to generate a range in total score from 0–17 points.

Histological assessment of colitis. Histological scoring was performed on the basis of 3 parameters as previously described[30] the severity of inflammation, crypt damage and ulceration. Each parameter was scored as follows: inflammation: rare inflammatory cells in the lamina propria (score 0), increased numbers of granulocytes in the lamina propria (1 point), confluence of inflammatory cells extending into the submucosa (2 points), and transmural extension of the inflammatory infiltrate (3 points); crypt damage: intact crypts (0 points), loss of the basal one-third (1 point), loss of the basal two-thirds (2 points), entire crypt loss (3 points), a change of epithelial surface with erosion (4 points), and confluent erosion (5 points); ulceration: an absence of ulcer (0 points), 1 or 2 foci of ulcerations (1 point), 3 or 4 foci of ulcerations (2 points), and confluent or extensive ulceration (3 points). These values were totaled to give a score range of 0–11 points. A minimum of three sections of the colon per animal were scored.

Isolation of total colonic cells for flow cytometry analysis. Isolation of colonic cells was performed. Briefly, large intestine were excised and opened longitudinally, washed of fecal contents, cut into pieces 0.5 cm in length, and subjected to two sequential 20-minute incubations in HBSS with 5% FBS and 2 mmol/l EDTA at 37 °C with agitation. After each incubation step, media containing debris was discarded. The remaining tissue was minced and incubated for 11 minutes in HBSS with 5% FBS, 1.5 mg/ml collagenase VIII (Sigma-Aldrich), and 40 U/ml DNase I (Roche Diagnostics, Indianapolis, IN) at 37 °C in agitation. Cell suspensions were collected and passed through a 100-µm strainer and pelleted by centrifugation at 300 g. To perform flow cytometry analysis, the antibodies below were used.

Flow cytometry analysis. Antibodies and reagents. The following antibodies were used: CD45-PerCP (30F11; BD), Alexa Fluor 647-conjugated CD98 (Biolegend; clone RL388), CD11c-allophycocyanin (N418; eBioscience), MHC II (I-Ab)–Alexa Fluor 700 (M5/114.15.2; eBioscience), CD11b–eFluor 450 (M1/70; eBioscience), and F4/80–PE-Cy7 (BM8; eBioscience). Dead cells were identified using the fixable Aqua Dead Cell Staining Kit (Invitrogen).

Purification of RNA extracted from mice after DSS treatment. DSS was shown to block the different enzymatic step of qPCR.[50] We thus extracted purified RNA according to the protocol described by Viennois *et al.*[50].

Statistical analysis. Data are presented as average values and standard deviations from experiments performed in triplicate ($n = 3$), except for cytotoxicity tests and *in vivo* experiments ($n = 8$). Analysis of variance tests were performed to obtain statistical comparisons between samples.

Materials. Branched PEI (M_n = 1,800 g/mol, M_w = 2,000 g/mol), PLA (M_w = 75–120 kg/mol) from Aldrich Chemistry (St Louis, MO). Alexa Fluor 568 phalloidin (M_w = 1,590), 4′,6-diamidino-2-phenyl-indole dihydrochloride (DAPI) and fluorescently tagged siRNA (Block-it fluorescent control) were obtained from Invitrogen (Eugene, OR). The cell proliferation reagent, WST-1, was purchased from Roche Diagnostics. PVA (86–89% hydrolyzed, low molecular weight) was purchased from Alfa Aesar (Ward Hill, MA). Silencer negative control and CD98 silencer predesigned siRNA were acquired from Sigma-Aldrich.

Revere phase high performance liquid chromatography. See "Supplementary materials and methods"

SUPPLEMENTARY MATERIAL

Figure S1. Internalization of FITC-tagged siRNA-loaded nanoparticles (NPs) in macrophages cells.

Figure S2. Absence of dissemination of NPs subproducts of degradation (lactic acid) in mice serum treated with nanoparticles (NPs).

Figure S3. Uptake of FITC-tagged siRNA-loaded NPs in different colonic cells types from mice explant treated with nanoparticles (NPs). **Materials and Methods.**

ACKNOWLEDGMENTS

We dedicate this article to the memory of Shanthi V Sitaraman, a brilliant scientist, dedicated physician, passionate humanitarian and dearest friend. This work was supported by grants from the Department of Veterans Affairs and the National Institutes of Health of Diabetes and Digestive and Kidney by the grant RO1-DK-071594 (to D.M), K01-DK-097192 (to H.L.) and B.X. is a recipient of an American Heart Association (AHA) postdoctoral fellowship. The authors declare no conflict of interest.

REFERENCES

1. Toruner, M, Loftus, EV Jr, Harmsen, WS, Zinsmeister, AR, Orenstein, R, Sandborn, WJ *et al.* (2008). Risk factors for opportunistic infections in patients with inflammatory bowel disease. *Gastroenterology* **134**: 929–936.
2. Dignass, A, Van Assche, G, Lindsay, JO, Lémann, M, Söderholm, J, Colombel, JF *et al.*; European Crohn's and Colitis Organisation (ECCO). (2010). The second European evidence-based Consensus on the diagnosis and management of Crohn's disease: Current management. *J Crohns Colitis* **4**: 28–62.
3. Xue, FM, Zhang, HP, Hao, HJ, Shi, ZY, Zhou, C, Feng, B *et al.* (2012). CD98 positive eosinophils contribute to T helper 1 pattern inflammation. *PLoS ONE* **7**: e51830.
4. Nguyen, HT, Dalmasso, G, Torkvist, L, Halfvarson, J, Yan, Y, Laroui, H *et al.* (2011). CD98 expression modulates intestinal homeostasis, inflammation, and colitis-associated cancer in mice. *J Clin Invest* **121**: 1733–1747.
5. Feral, CC, Nishiya, N, Fenczik, CA, Stuhlmann, H, Slepak, M and Ginsberg, MH (2005). CD98hc (SLC3A2) mediates integrin signaling. *Proc Natl Acad Sci USA* **102**: 355–360.
6. Prager, GW, Féral, CC, Kim, C, Han, J and Ginsberg, MH (2007). CD98hc (SLC3A2) interaction with the integrin beta subunit cytoplasmic domain mediates adhesive signaling. *J Biol Chem* **282**: 24477–24484.
7. Fais, S and Pallone, F (1989). Ability of human colonic epithelium to express the 4F2 antigen, the common acute lymphoblastic leukemia antigen, and the transferrin receptor. Studies in inflammatory bowel disease and after *in vitro* exposure to different stimuli. *Gastroenterology* **97**: 1435–1441.
8. Yan, Y, Dalmasso, G, Sitaraman, S and Merlin, D (2007). Characterization of the human intestinal CD98 promoter and its regulation by interferon-gamma. *Am J Physiol Gastrointest Liver Physiol* **292**: G535–G545.
9. Nguyen, HT, Dalmasso, G, Yan, Y, Laroui, H, Dahan, S, Mayer, L *et al.* (2010). MicroRNA-7 modulates CD98 expression during intestinal epithelial cell differentiation. *J Biol Chem* **285**: 1479–1489.
10. Tsumura, H, Ito, M, Li, XK, Nakamura, A, Ohnami, N, Fujimoto, J *et al.* (2012). The role of CD98hc in mouse macrophage functions. *Cell Immunol* **276**: 128–134.
11. Kucharzik, T, Lugering, A, Yan, Y, Driss, A, Charrier, L, Sitaraman, S *et al.* (2005). Activation of epithelial CD98 glycoprotein perpetuates colonic inflammation. *Lab Invest* **85**: 932–941.
12. Lieberman, J, Song, E, Lee, SK and Shankar, P (2003). Interfering with disease: opportunities and roadblocks to harnessing RNA interference. *Trends Mol Med* **9**: 397–403.
13. Meade, BR and Dowdy, SF (2007). Exogenous siRNA delivery using peptide transduction domains/cell penetrating peptides. *Adv Drug Deliv Rev* **59**: 134–140.
14. Kim, B, Tang, Q, Biswas, PS, Xu, J, Schiffelers, RM, Xie, FY *et al.* (2004). Inhibition of ocular angiogenesis by siRNA targeting vascular endothelial growth factor pathway genes: therapeutic strategy for herpetic stromal keratitis. *Am J Pathol* **165**: 2177–2185.
15. Pardridge, WM (2004). Intravenous, non-viral RNAi gene therapy of brain cancer. *Expert Opin Biol Ther* **4**: 1103–1113.
16. Toub, N, Bertrand, JR, Tamaddon, A, Elhamess, H, Hillaireau, H, Maksimenko, A *et al.* (2006). Efficacy of siRNA nanocapsules targeted against the EWS-Fli1 oncogene in Ewing sarcoma. *Pharm Res* **23**: 892–900.
17. Fattal, E, Vauthier, C, Aynie, I, Nakada, Y, Lambert, G, Malvy, C *et al.* (1998). Biodegradable polyalkylcyanoacrylate nanoparticles for the delivery of oligonucleotides. *J Control Release* **53**: 137–143.
18. Laroui, H, Theiss, AL, Yan, Y, Dalmasso, G, Nguyen, HT, Sitaraman, SV *et al.* (2011). Functional TNFa gene silencing mediated by polyethyleneimine/TNFa siRNA nanocomplexes in inflamed colon. *Biomaterials* **32**: 1218–1228.
19. Lamprecht, A, Schäfer, U and Lehr, CM (2001). Size-dependent bioadhesion of micro- and nanoparticulate carriers to the inflamed colonic mucosa. *Pharm Res* **18**: 788–793.
20. Mao, S, Neu, M, Germershaus, O, Merkel, O, Sitterberg, J, Bakowsky, U *et al.* (2006). Influence of polyethylene glycol chain length on the physicochemical and biological properties of poly(ethylene imine)-graft-poly(ethylene glycol) block copolymer/SiRNA polyplexes. *Bioconjug Chem* **17**: 1209–1218.
21. Jere, D, Jiang, HL, Arote, R, Kim, YK, Choi, YJ, Cho, MH *et al.* (2009). Degradable polyethylenimines as DNA and small interfering RNA carriers. *Expert Opin Drug Deliv* **6**: 827–834.
22. Abbasi, S, Paul, A and Prakash, S (2011). Investigation of siRNA-loaded polyethylenimine-coated human serum albumin nanoparticle complexes for the treatment of breast cancer. *Cell Biochem Biophys* **61**: 277–287.
23. Höbel, S, Prinz, R, Malek, A, Urban-Klein, B, Sitterberg, J, Bakowsky, U *et al.* (2008). Polyethylenimine PEI F25-LMW allows the long-term storage of frozen complexes as fully active reagents in siRNA-mediated gene targeting and DNA delivery. *Eur J Pharm Biopharm* **70**: 29–41.
24. Charrier, L, Yan, Y, Driss, A, Laboisse, CL, Sitaraman, SV and Merlin, D (2005). ADAM-15 inhibits wound healing in human intestinal epithelial cell monolayers. *Am J Physiol Gastrointest Liver Physiol* **288**: G346–G353.
25. Charrier, L, Yan, Y, Nguyen, HT, Dalmasso, G, Laboisse, CL, Gewirtz, AT *et al.* (2007). ADAM-15/metargidin mediates homotypic aggregation of human T lymphocytes and heterotypic interactions of T lymphocytes with intestinal epithelial cells. *J Biol Chem* **282**: 16948–16958.
26. Maruyama, K, Iwasaki, F, Takizawa, T, Yanagie, H, Niidome, T, Yamada, E *et al.* (2004). Novel receptor-mediated gene delivery system comprising plasmid/protamine/sugar-containing polyanion ternary complex. *Biomaterials* **25**: 3267–3273.
27. Akinc, A, Thomas, M, Klibanov, AM and Langer, R (2005). Exploring polyethylenimine-mediated DNA transfection and the proton sponge hypothesis. *J Gene Med* **7**: 657–663.
28. Laroui, H, Dalmasso, G, Nguyen, HT, Yan, Y, Sitaraman, SV and Merlin, D (2010). Drug-loaded nanoparticles targeted to the colon with polysaccharide hydrogel reduce colitis in a mouse model. *Gastroenterology* **138**: 843–53.e1.
29. Yan, Y, Kolachala, V, Dalmasso, G, Nguyen, H, Laroui, H, Sitaraman, SV *et al.* (2009). Temporal and spatial analysis of clinical and molecular parameters in dextran sodium sulfate induced colitis. *PLoS ONE* **4**: e6073.
30. Cooper, HS, Murthy, SN, Shah, RS and Sedergran, DJ (1993). Clinicopathologic study of dextran sulfate sodium experimental murine colitis. *Lab Invest* **69**: 238–249.
31. Stallmach, A, Hagel, S and Bruns, T (2010). Adverse effects of biologics used for treating IBD. *Best Pract Res Clin Gastroenterol* **24**: 167–182.
32. Nguyen, HT, Dalmasso, G, Yan, Y, Laroui, H, Charania, M, Ingersoll, S *et al.* (2012). Intestinal epithelial cell-specific CD98 expression regulates tumorigenesis in Apc(Min/+) mice. *Lab Invest* **92**: 1203–1212.
33. Charania, MA, Ayyadurai, S, Ingersoll, SA, Xiao, B, Viennois, E, Yan, Y *et al.* (2012). Intestinal epithelial CD98 synthesis specifically modulates expression of colonic microRNAs during colitis. *Am J Physiol Gastrointest Liver Physiol* **302**: G1282–G1291.
34. deShazo, RD and Kemp, SF (1997). Allergic reactions to drugs and biologic agents. *JAMA* **278**: 1895–1906.
35. Riedl, MA and Casillas, AM (2003). Adverse drug reactions: types and treatment options. *Am Fam Physician* **68**: 1781–1790.
36. Tiemi, J, Komati, S and Sdepanian, VL (2010). Effectiveness of infliximab in Brazilian children and adolescents with Crohn disease and ulcerative colitis according to clinical manifestations, activity indices of inflammatory bowel disease, and corticosteroid use. *J Pediatr Gastroenterol Nutr* **50**: 628–633.
37. Tursi, A, Elisei, W, Brandimarte, G, Giorgetti, G, Penna, A and Castrignano, V (2010). Safety and effectiveness of infliximab for inflammatory bowel diseases in clinical practice. *Eur Rev Med Pharmacol Sci* **14**: 47–55.
38. Miele, E, Markowitz, JE, Mamula, P and Baldassano, RN (2004). Human antichimeric antibody in children and young adults with inflammatory bowel disease receiving infliximab. *J Pediatr Gastroenterol Nutr* **38**: 502–508.
39. Schneeweiss, S, Korzenik, J, Solomon, DH, Canning, C, Lee, J and Bressler, B (2009). Infliximab and other immunomodulating drugs in patients with inflammatory bowel disease and the risk of serious bacterial infections. *Aliment Pharmacol Ther* **30**: 253–264.
40. Biancone, L, Petruzziello, C, Orlando, A, Kohn, A, Ardizzone, S, Daperno, M *et al.* (2011). Cancer in Crohn's Disease patients treated with infliximab: a long-term multicenter matched pair study. *Inflamm Bowel Dis* **17**: 758–766.
41. Iborra, M, Beltrán, B, Bastida, G, Aguas, M and Nos, P (2011). Infliximab and adalimumab-induced psoriasis in Crohn's disease: a paradoxical side effect. *J Crohns Colitis* **5**: 157–161.
42. Wachsmann, P and Lamprecht, A (2012). Polymeric nanoparticles for the selective therapy of inflammatory bowel disease. *Meth Enzymol* **508**: 377–397.
43. Namba, K, Nishio, M, Mori, K, Miyamoto, N, Tsurudome, M, Ito, M *et al.* (2001). Involvement of ADAM9 in multinucleated giant cell formation of blood monocytes. *Cell Immunol* **213**: 104–113.
44. Helming, L and Gordon, S (2007). The molecular basis of macrophage fusion. *Immunobiology* **212**: 785–793.
45. MacLauchlan, S, Skokos, EA, Meznarich, N, Zhu, DH, Raoof, S, Shipley, JM *et al.* (2009). Macrophage fusion, giant cell formation, and the foreign body response require matrix metalloproteinase 9. *J Leukoc Biol* **85**: 617–626.
46. Ferrés-Coy, A, Pilar-Cuellar, F, Vidal, R, Paz, V, Masana, M, Cortés, R *et al.* (2013). RNAi-mediated serotonin transporter suppression rapidly increases serotonergic neurotransmission and hippocampal neurogenesis. *Transl Psychiatry* **3**: e211.
47. Li, L, Wang, R, Wilcox, D, Zhao, X, Song, J, Lin, X *et al.* (2012). Tumor vasculature is a key determinant for the efficiency of nanoparticle-mediated siRNA delivery. *Gene Ther* **19**: 775–780.
48. Ngamwongsatit, P, Banada, PP, Panbangred, W and Bhunia, AK (2008). WST-1-based cell cytotoxicity assay as a substitute for MTT-based assay for rapid detection of toxigenic Bacillus species using CHO cell line. *J Microbiol Methods* **73**: 211–215.
49. Pizarro, TT, Arseneau, KO, Bamias, G and Cominelli, F (2003). Mouse models for the study of Crohn's disease. *Trends Mol Med* **9**: 218–222.
50. Viennois, E, Chen, F, Laroui, H, Baker, MT and Merlin, D (2013). Dextran sodium sulfate inhibits the activities of both polymerase and reverse transcriptase: lithium chloride purification, a rapid and efficient technique to purify RNA. *BMC Res Notes* **6**: 360.